

H01/5

ULTIMATE STRENGTH OF REINFORCED CONCRETE MEMBERS SUBJECTED TO TRANSIENT HIGH TEMPERATURE DISTRIBUTION

H. Saito, M. Hiramoto, K. Saito, T. Miyashita, Y. Takeuchi and T. Mochida

1. INTRODUCTION

In order to assure the safety of an RCCV in a severe accident beyond its assumed design limits, it is necessary to establish an estimation method of the ultimate strength of the RCCV in severe conditions, such as it would receive under heavy internal pressure in a markedly elevated atmospheric temperature. The non linear finite element analysis which takes into proper account the alteration of the mechanical properties of concrete and the reinforcing bars due to the elevated temperature seems to be an effective method. However, there are only a few experimental data available at present to examine the propriety of these analytical methods.

This study was plotted to examine the fundamental properties of RC members subjected to an elevated surface temperature through a loading test reflecting the condition of a severe accident to an RCCV.

Through the test, many useful experimental data were obtained to examine the availability of an analytical method for estimating the ultimate strength of an RCCV in a severe accident. An estimation method of the ultimate strength of RC deep beams subjected to elevated surface temperatures was also proposed in this paper.

2. OUTLINE OF LOADING TEST

As shown in Table 1, the loading tests in the SC, ST and the F series, reflecting the condition of a severe accident, were carried out with the RC beam specimens which had identical cross section sizes. S00 and F00 were specimens to be loaded under room temperature.

Specimens in the SC series had a shear span ratio of 0.75, and these were loaded to be compressed on a heated surface. Specimens in the ST series had the same shear span ratio as the SC series, and these were loaded to be tensioned on a heated surface. These specimens in the SC or the ST series were a type of deep beams. The specimens in the F series were beams with a shear span ratio of 2 and were loaded to be compressed on a heated surface. A surface temperature of 300°C or 800°C (600°C for ST series) was applied in each of the test series.

Details of the specimens for the SC series are shown in Fig.1. The depth of the specimens corresponded to a 1/2.5 wall thickness of a full scale RCCV. To measure the strain of the reinforcing bars in the region of the elevated temperatures a special type of strain gauges enclosed in a capsule was used.

The upper surface of the specimens was heated and the surface temperature was controlled to be raised at a constant speed by means of electric panel heaters set on the specimens. Ceramic fibers with a thickness of 100 mm were installed on the sides of the specimens.

The following simplified test procedure was adopted to make easier the comparison of the test results with an analytical result. That is, first the surface temperature was raised up to a specified level at a speed of 10°C/hr or 13°C/hr, which was one of the anticipated temperature rises in a severe accident, allowing the thermal deflection to be developed freely and then an external load was applied monotonously by oil jacks to the specimens supported by a pair of pin and pin-roller shoes up to their failure keeping the surface temperature at the specified level.

The experimental system for the SC series are shown in Fig.2. The deflections of the specimens at the mid span, temperatures inside the specimens and the strains of the reinforcing bars were measured.

Table 2 shows the test results of the mechanical properties of the reinforcing bars. The tests for the mechanical properties of the reinforcing bars and the concrete were conducted under room temperature.

3. TEST RESULTS

Figure 3 illustrates the isothermal lines in the SC and the ST series while an external load was applied. In the vicinity of the loaded point, the heat dissipated through the loading apparatus, resulting in a smaller temperature rise and an uneven temperature distribution in the axial direction.

Test results for the shear or flexural crack initiating loads are summarized in Table 3. Crack initiating loads were judged from the observed strain behavior of the shear or tension reinforcement bars. Crack initiating loads visually observed for S00 and F00 are shown in parentheses, and they correspond well with those judged from the observed strains. Crack initiating loads were reduced with the increase of the surface temperature.

Figure 4 compares the load-deflection relationship in the SC, ST series and in the F series to examine the influence of the surface temperature on the rigidity and on the ultimate strength, adjusting the deflections at the beginning of loading equaling to zero.

The load-deflection relationship in the S3C represented almost the same relationship with that of the S00 which collapsed abruptly by shear failure, while the S8C resulted in a marked reduction compared with the S00, both in the rigidity and in the ultimate strength, and they also lost the load carrying ability by shear failure.

In the case of the ST series, the rigidity and the ultimate strength of the S3T decreased a little more than those of the S3C, while those of the S6T were greatly decreased due to the elevated temperature. They also lost the load carrying capacity by shear failure.

In the case of the F00, shear cracks, as well as flexural cracks, developed gradually with an increase in the load, and finally it lost the load carrying capacity by shear failure due to an increase in the shear crack widths. The collapsing process for the F3C and the F8C was imagined to be nearly the same as that for the F00, and the rigidity of these specimens decreased in proportion to the surface temperature. The ultimate strength of the F8C was reduced to 90 % of the F00, while that of the F3C slightly exceeded the F00.

The observed cracks in the S00 and the S8C after their failure, and those in the F00 and the F8C, are illustrated in Fig.5. In the heated specimens, along with the flexural and the shear cracks, vertical cracks were found for the member axis at a certain interval and fine cracks were observed near the heated surface. These cracks were probably caused by thermal effects such as an internal restraining stress, drying shrinkage of concrete, or the difference between the thermal expansion coefficient of the reinforcements and of the concrete during the rise in temperature. To distinguish them from the flexural or shear cracks, they are shown as broken lines in the figure.

The load-strain relations of the longitudinal reinforcements in the SC and the ST series are shown in Fig.6. The strain of the tension reinforcements in the SC series or the compression reinforcements in the ST series resulted in nearly the same relationship at any surface temperature. On the other hand,

that of the compression reinforcements in the SC series or the tension reinforcements in the ST series were affected remarkably by the surface temperature. This revealed that the flexural rigidity of the RC members was determined by the material characteristics of the concrete and the longitudinal reinforcements in the range of the high temperature.

4. EXAMINATION OF THE ULTIMATE STRENGTH

In this section a method is shown for estimating the ultimate strength of the RC members subjected to an elevated surface temperature.

The objects of the examination were deep beam-type specimens in the SC and the ST series. The ultimate strength of these specimens was evaluated using a formula for calculating the maximum strength of the deep beams, taking into account the reduction of the material properties such as the compressive strength of concrete, the yield point and Young's modulus for the reinforcing bars under the influence of an elevated temperature.

The formula used as a base for the examination was Niwa's formula¹⁾ which represented the shear strength of the deep beams without the shear reinforcement in Eq.(1).

$$V_c = 0.53 f_c' \cdot \sqrt[3]{b d} (1 + 3.33 r / d) (1 + \sqrt{Pt}) / \{1 + (a / d)^2\} \quad (1)$$

In this, f_c' : compressive strength of concrete; b : section width; d : distance from extreme compression fiber to centroid of tension reinforcement; r : width of a bearing plate; Pt : ratio of tension reinforcement (%); a : shear span.

The shear strength of the deep beams with the shear reinforcement can be evaluated in Eq.(2) by the sum of the shear strength provided by the shear reinforcement, which was calculated by the truss theory and that given by Niwa's formula.

$$V = V_c + A_w \cdot f_{wy} \cdot j / s \quad (2)$$

In this, A_w : area of shear reinforcement within a distance s ; f_{wy} : yield point of shear reinforcement; j : distance between center of tension and compression in a section ($j=d/1.15$); s : spacing of shear reinforcement.

f_c' in Eq.(1) was reduced to the strength corresponding to the temperature near the loading point, which was shown in a circle on the isothermal line in Fig.3, assuming that the shear strength was determined by the compressive strength of the concrete near the loading point. The reduction of Young's modulus of the tension reinforcement at an elevated temperature was also considered in Eq.(1) as the decrease of Pt . The shear strength provided by the shear reinforcement was estimated taking into account the reduction of the yield point of the shear reinforcement due to the temperature near the heated side.

The reduction of these material properties due to the elevated temperature was determined based on the test data conducted by a related study²⁾ (See Figure 7).

The estimated shear strength and the flexural strength are shown in Fig.8 compared with the ultimate strength of the test results. The flexural strength Q_m was calculated in Eq.(3), taking into account the reduction of the yield point of the tension reinforcement at the elevated temperature.

$$Q_m = 0.9 A_s \cdot f_y \cdot d / a \quad (3)$$

In this, A_s : area of tension reinforcement; f_y : yield point of tension reinforcement.

The test results in the SC series agreed well with the estimated shear strengths which determined the ultimate strength of the specimens in the SC series. The test results in the ST series also corresponded fairly well with the estimated shear strengths which were comparable to the flexural strength in this case.

5. CONCLUSION

As a result of the loading tests with the RC beam specimens in the 3 test series, reflecting the condition of a severe accident to an RCCV, it was clarified that the surface temperature exerted much influence on the fundamental properties of the RC members such as the rigidity, crack initiating load and the ultimate strength. Through the test, many useful data were obtained to examine the propriety of an analytical method of estimating the ultimate strength of an RCCV in a severe accident.

The examination of the test results showed that it was possible to find the ultimate strength of the RC deep beams subjected to elevated surface temperatures by applying a formula for the deep beams, if the reduction of material properties such as the compressive strength of concrete, the yield point and Young's modulus for the reinforcing bars under the influence of an elevated temperature was properly taken into account.

ACKNOWLEDGEMENT

This paper is a part of the results of a joint research study conducted by Tokyo Electric Power Company, Tohoku Electric Power Company, Chubu Electric Power Company, Hokuriku Electric Power Company, Chugoku Electric Power Company, The Japan Atomic Power Company, Hitachi Limited, Toshiba Corporation, Kajima Corporation, Shimizu Corporation and Takenaka Corporation.

REFERENCE

- 1)Niwa. J.,1983, Equation for Shear Strength of Reinforced Concrete Deep Beams Based on FEM Analysis, Proceedings of JCI 2nd Colloquium on Shear Analysis of RC Structures, (in Japanese).
- 2)Takeuchi,M.,et.al.,Material Properties of Concrete and Steel Bars at Elevated Temperatures, 1993, 12th SMIRT, Vol.H

Table 1 Description of Specimens and Test Conditions

Test Series	Specimen	Concrete		Tension Reinforcement		Shear Reinforcement		Shear Span Ratio	Surface Temperature °C	Heated Surface
		Compressive Strength f_c' kgf/cm ²	Young's Modulus E_c kgf/cm ²	Arrangement	Pt %	Arrangement	Pw %			
SC	S00	288	2.61×10^5	12-D25	1.52	D10 @150	0.19	0.75	Room Temp. 300 800	Compression Side
	S3C									
	S8C									
ST	S3T	287	2.81×10^5	12-D25	1.52	D10 @150	0.19	0.75	300 600	Tension Side
	S6T									
F	F00	303	2.53×10^5	10-D22	0.97	D10 @150	0.19	2.0	Room Temp. 300 800	Compression Side
	F3C									
	F8C									

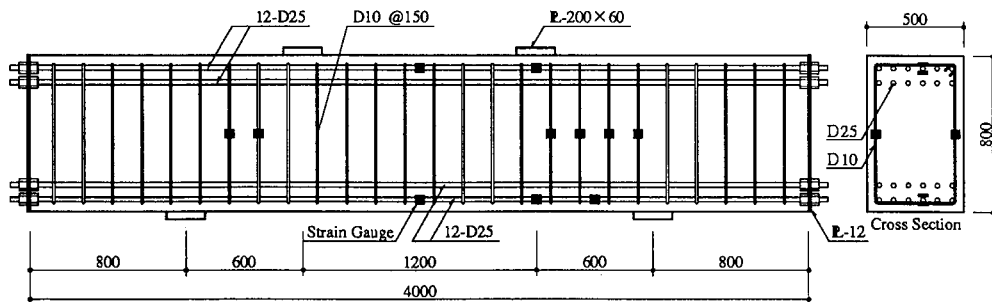


Fig. 1 Details of Specimens for SC Series

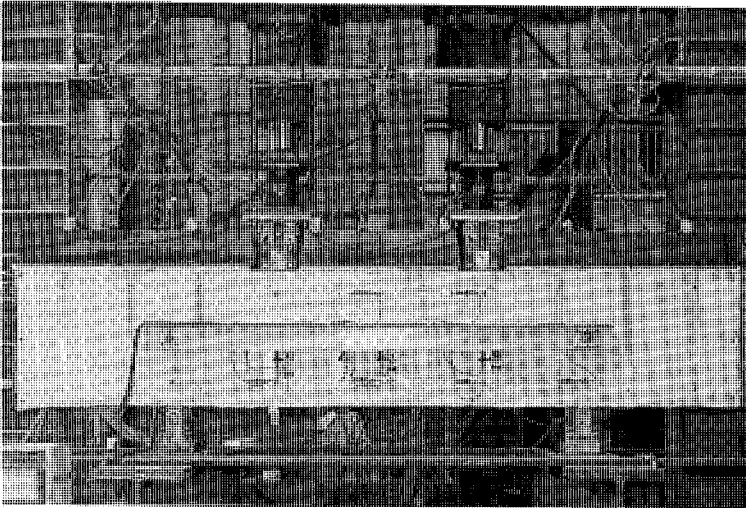


Fig. 2 Experimental System for SC Series

Table 2 Mechanical Properties of Reinforcing bars

Designation	Yield Point f_y kgf/cm ²	Tensile Strength kgf/cm ²	Young's Modulus E_s kgf/cm ²	Elongation %
D10	3636	5038	1.96×10^6	24
D22	4122	5871	2.07×10^6	25
D25	4108	5907	2.08×10^6	31

Table 3 Crack Initiating Load and Ultimate Strength

Test Series	Specimen	Crack Initiating Load		Ultimate Strength
		Flexural Crack	Shear Crack	
SC	S00	56 (41)	71 (83)	231.4
	S3C	46	58	226.7
	S8C	31	33	177.0
ST	S3T	—	86	209.0
	S6T	—	22	180.3
F	F00	18(17.5)	35(35.5)	67.5
	F3C	9	28	69.8
	F8C	9	17	59.4

unit : tonf

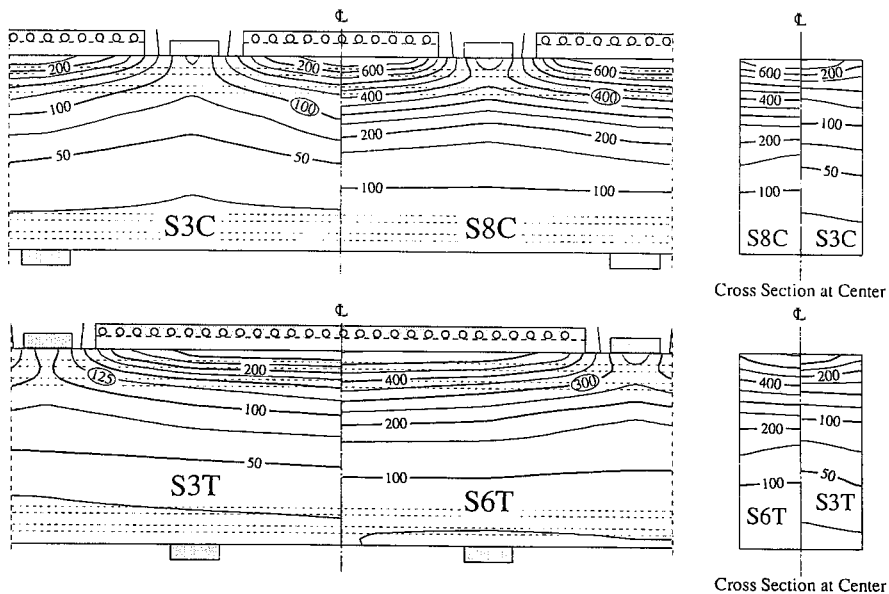


Fig. 3 Isothermal Lines during Loading

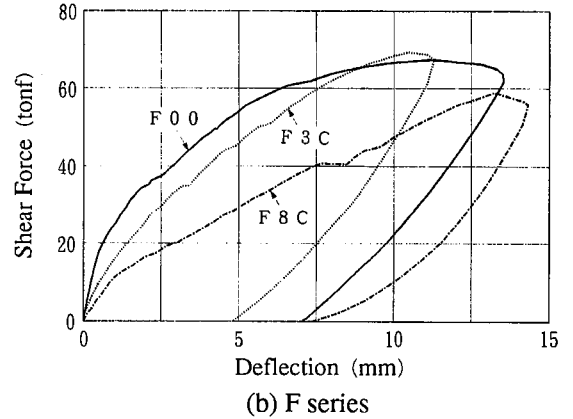
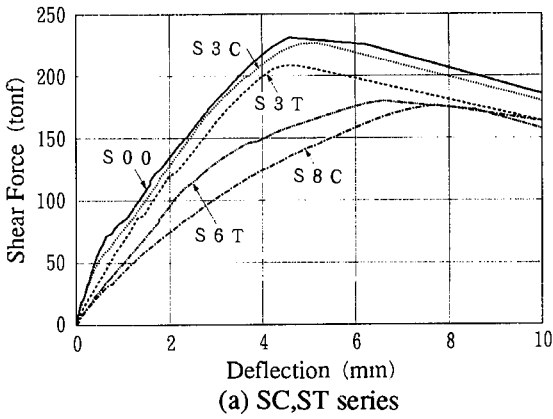


Fig. 4 Load-Deflection Relationship

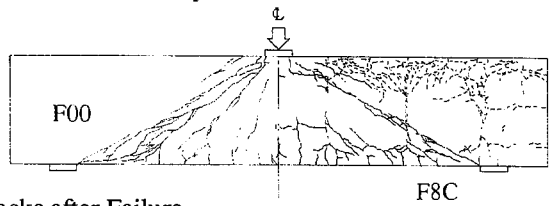
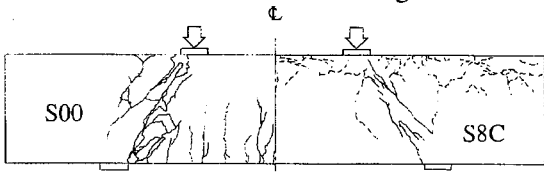


Fig. 5 Observed Cracks after Failure

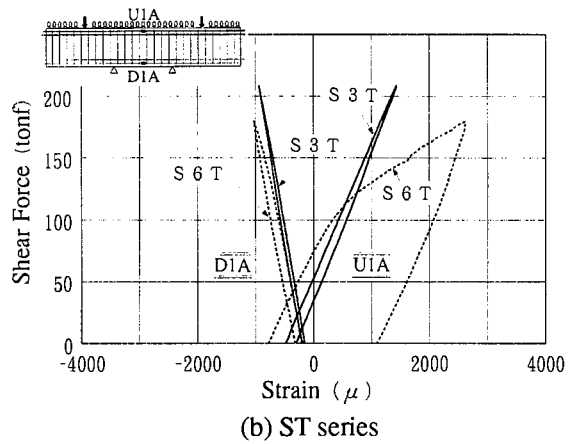
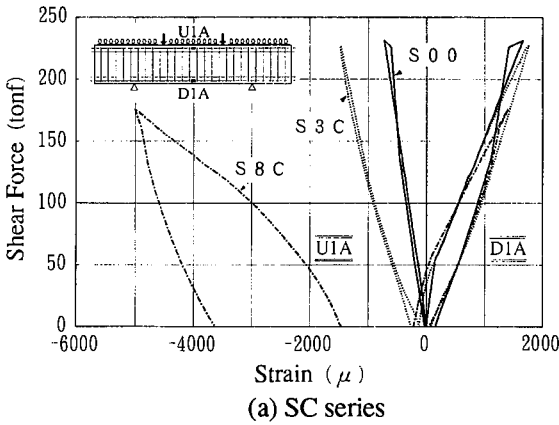


Fig. 6 Load vs. Strain of Longitudinal Reinforcement

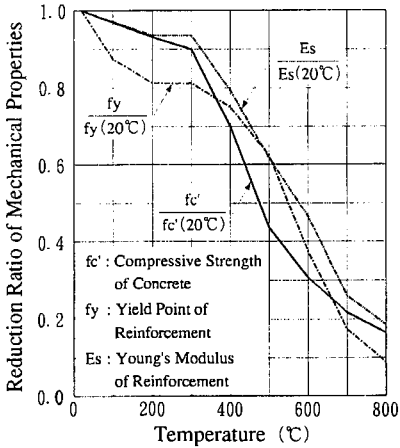


Fig. 7 Dependence of Mechanical Properties with respect to Temperature

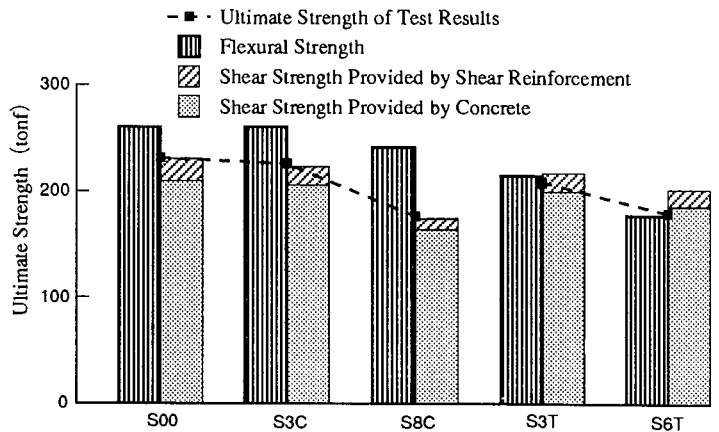


Fig. 8 Comparison of Ultimate Strength between Test and Calculated Results